Combined influence of oceanic and atmospheric circulations on Greenland Sea Ice concentration

Sourav Chatterjee[1,2]*, Roshin P Raj[3], Laurent Bertino[3], Sebastian H. Mernild[3], Subeesh MP[1], Nuncio Murukesh[1], Muthalagu Ravichandran[1]

[1]National Centre for Polar and Ocean Research, Ministry of Earth Sciences, India

[2] School of Earth, Ocean and Atmospheric Sciences, Goa University, India

[3]Nansen Environmental and Remote Sensing Center and Bjerknes Centre for Climate Research, Bergen, Norway

Corresponds to: Sourav Chatterjee (sourav@ncpor.res.in)

Abstract.

The amount and spatial extent of Greenland Sea (GS) ice are primarily controlled by the sea ice export across the Fram Strait (FS) and by local seasonal sea ice formation, melting, and sea ice dynamics. In this study, using satellite passive microwave sea ice observations, atmospheric and a coupled ocean-sea ice reanalysis system, TOPAZ4, we show that both the atmospheric and oceanic circulation in the Nordic Seas (NS) act in tandem to explain the SIC variability in the western GS. Northerly wind anomalies associated with anomalous low SLP over the NS reduce the sea ice export in the western GS due to westward Ekman drift of sea ice. On the other hand, the positive wind stress curl strengthens the cyclonic Greenland Sea Gyre (GSG) circulation in the central GS. An intensified GSG circulation may result in stronger Ekman divergence of surface cold and fresh waters away from the western GS. Both of these processes can reduce the freshwater content and weaken the upper ocean stratification in the western GS. At the same time, warm and saline Atlantic Water (AW) anomalies are recirculated from the FS region to western GS by a stronger GSG circulation. Under a weakly stratified condition, enhanced vertical mixing of these subsurface AW anomalies can warm the surface waters and inhibit new sea ice formation, further reducing the SIC in the western GS.

1 Introduction

The strength of the Atlantic meridional overturning circulation partly depends on freshwater availability in the GS (Serreze et al. 2007; Eldevik & Nilsen 2013; Buckley & Marshall 2016). The freshwater content in this region is largely driven by the amount of sea ice therein (Aagaard & Carmack 1989). Sea ice in GS is also important in determining shipping routes (Instanes et al. 2005; Johannessen et al. 2007), as well as to the regional marine ecosystem due to its impact on the light availability (Grebmeier et al. 1995). Most of the sea ice in the GS is exported from the central Arctic Ocean across the Fram Strait (FS) and is largely controlled by the ice-drift with the Transpolar Drift (Zamani et al. 2019). Anomalous sea ice export

through the FS is associated with events like the 'Great Salinity Anomaly' (Dickson et al. 1988) which can have impact on the freshwater content in the Nordic Seas. Therefore, it is quite evident that the changes in sea ice export through the FS influence the GS sea ice and thus the freshwater availability in the Nordic Seas (Belkin et al. 1998; Dickson et al. 1988; Serreze et al. 2006).

Even though it is one of the main mechanisms contributing to the overall SIC in GS, the relation between sea ice export through FS and SIC variability in GS is not very robust (Kern et al. 2010). This further points to the importance of local sea ice formation and sea ice dynamics in the GS. The impact of these processes can be realized prominently in the marginal ice zone (MIZ) in the western GS and the 'Odden' region in central GS (see Fig. 1 for approximate locations of the regions). These regions exhibit strong negative SIC trends during recent decades (Fig. 1a in Selyuzhenok et al. 2020). In fact, the central GS has been mostly ice free in recent years (Rogers and Hung, 2008, Moore et al., 2015) which has large implications on the open ocean convection in the central GS e.g limiting the formation of deep waters (Brakstad et al., 2019). Changes in sea ice of this region can modify the deep water convection through influencing both the heat and salt budgets (Shuchman et al. 1998). Selyuzhenok et al. (2020) found that in spite of increasing sea ice export through the FS, the overall sea ice volume (SIV) in the GS has been decreasing during the period 1979–2016. They further attributed the interannual variability and decreasing trend of SIV to local oceanic processes, more precisely warmer AW temperatures in the Nordic Seas. Further local meteorological parameters e.g. air temperature, wind speed and direction along with oceanic waves, eddies have also been found to influence the sea ice properties in the central GS, particularly for the Odden region (Campbell et al. 1987; Johannessen et al. 1987; Wadhams et al. 1996; Shuchman et al. 1998; Toudal 1999; Comiso et al., 2001).

Besides the local factors, sea ice in the GS also responds to large-scale atmospheric forcing. For example, a high sea level pressure (SLP) anomaly over the NS results in anomalous southerly wind in the GS. The associated Ekman drift towards the central GS may assist the eastward expansion of the sea ice and SIC increase in the central GS (Germe et al. 2011). Selyuzhenok et al. (2020) also argued that consistent positive North Atlantic Oscillation (NAO) forcing in recent decades have led to warmer AW waters in the NS and resulted in a declining SIV trend. However, the response of NS circulation to the atmospheric forcing and the mechanism through which it can influence the SIC in GS is not studied in detail.

The Greenland Sea Gyre (GSG) is a prominent feature of the subpolar North Atlantic ocean and can be intensified as a strong cyclonic circulation in the NS (Fig. 1). It is known to respond to the atmospheric forcing in the NS and contribute to AW heat distribution in the Nordic Seas (Hatterman et al. 2016; Chatterjee et al. 2018). A stronger GSG circulation increases the AW temperature in the FS by modifying the northward AW transport in its eastern side (Chatterjee et al. 2018). A simultaneous increase in its southward flowing western branch, constituting the southern recirculation pathway of AW (Hattermann et al. 2016; Jeansson et al. 2017), can increase the heat content in the western GS through a stronger and warmer recirculation of AW (Chatterjee et al. 2018). The return AW, even after significant modification, remains denser than the local cold and fresh surface waters and thus mostly remain in the subsurface (Schlichtholz & Houssais 1999;

Eldevik et al. 2009). However, enhanced vertical winter mixing can cause warming of the surface waters in the GS (Våge et al., 2018). Further, the eastward flowing Jan Mayen Current (JMC), originated from the East Greenland Current (EGC), constitutes the south-western closing branch of the cyclonic GSG circulation in the GS (Fig. 1b). The east-ward extension of the cold and fresh JMC into the central GS basin helps in both new sea ice formation and advection of sea ice from the EGC (Wadhams & Comiso 1999). Changes in GSG circulation and associated AW recirculation in GS may also influence the JMC strength and temperature. Thus given the potential role of GSG in modifying the oceanic conditions, it is important to understand how the response of GSG circulation to the atmospheric forcing can influence the SIC in the GS.

In this study we hypothesize that the interannual winter mean SIC variability in GS can be explained by the combined influence of atmospheric and oceanic circulations, more precisely the GSG circulation. Using a combination of satellite passive microwave SIC, a coupled sea ice ocean reanalysis and atmospheric reanalysis data, we show that changes in the GSG dynamics and resulting AW transport in GS can potentially influence the SIC in the western GS. Further, we also show that the atmospheric circulation associated with the GSG circulation variability provides the favourable conditions for the GSG's control on the SIC variability in the western GS region. Section 2 describes the data and methods applied in the study following the results in section 3. Discussions and conclusions are mentioned in section 4.

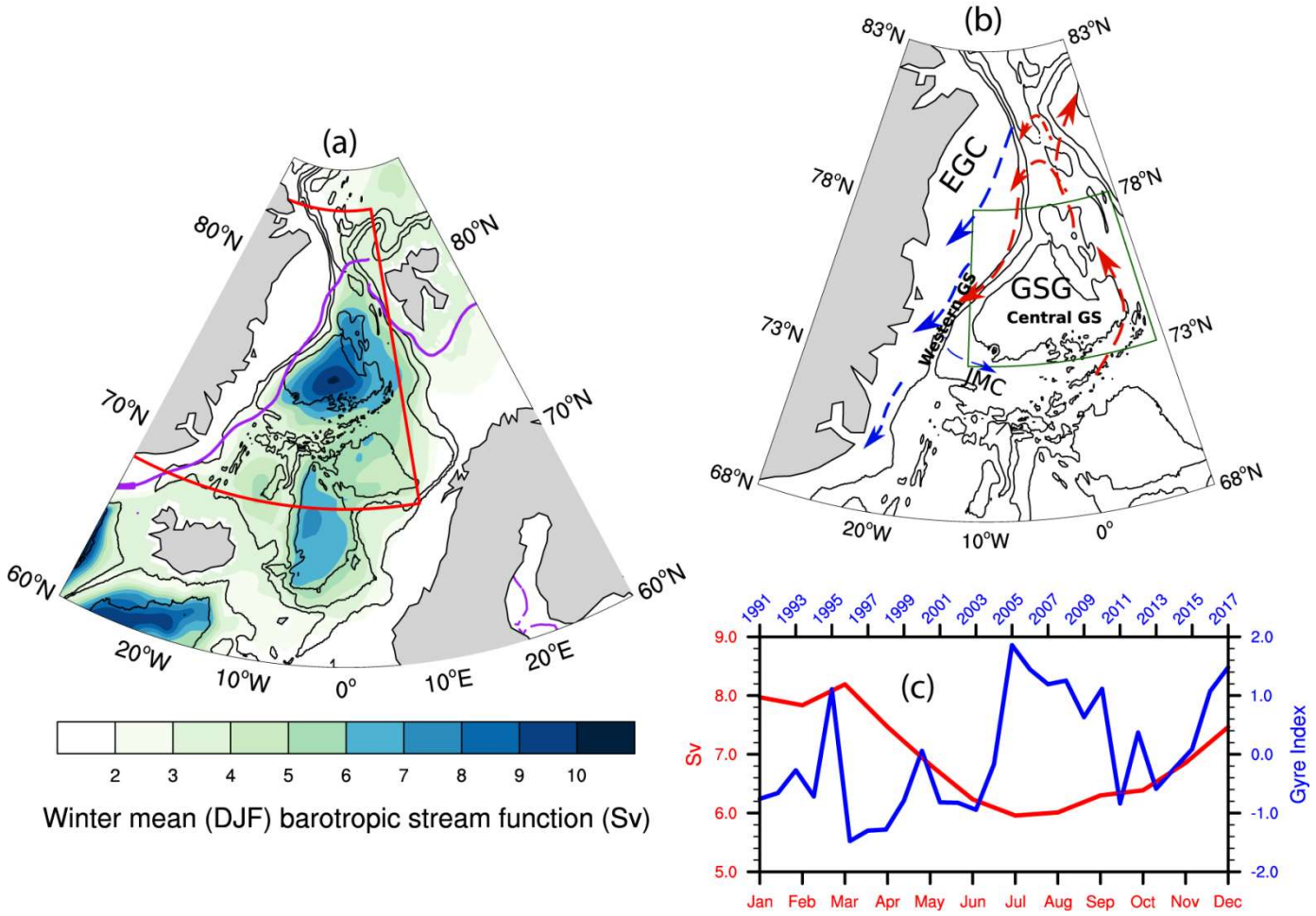

Figure 1: a) Winter mean (DJF) barotropic stream function for the period 1991–2017. The region marked in red indicates the Nordic Seas region. The purple line shows the mean DJF sea ice extent for the study period. b) Schematic of the major currents and discussed in the text. JMC: Jan Mayen Current; EGC: East Greenland Current; GSG: Greenland Sea Gyre. Warm currents are drawn in red and cold currents are in blue. Black contours are showing bottom topography drawn at every 1000 m. The thick black contour indicates the 3000m isobath. The marked region in dark green is used to calculate the 'gyre index' as detailed in the next section. c) The blue line indicates the gyre index used in this study and the red line shows the annual cycle of the strength of GSG circulation determined by averaging barotropic stream function within the 3000m isobath in the region marked in (b).

2. Data

2.1 Atmospheric data:

Monthly mean sea level pressure (SLP) data was obtained from the ERA Interim reanalysis (Dee et al. 2011) for the period 1991–2017 on a 0.5 by 0.5 degree grid resolution. Monthly anomalies were calculated from the monthly climatology field using the full time period (1991–2017) and were averaged for December-January-February (DJF). For the linear regression analysis the DJF averaged SLP anomalies were detrended.

2.2 Oceanic data:

Monthly mean oceanic data used in this study were taken from TOPAZ4, a coupled ocean and sea ice data assimilation system for the North Atlantic and the Arctic. TOPAZ4 is based on the Hybrid Coordinate Ocean Model (HYCOM, with 28 hybrid z-isopycnal layers at a horizontal resolution of 12 to 16 km in the Nordic Seas and the Arctic) and Ensemble Kalman Filter data assimilation, the results of which have been evaluated in earlier studies (Lien et al. 2016; Xie et al. 2017; Chatterjee et al. 2018; Raj et al. 2019). TOPAZ4 represents the Arctic component of the Copernicus Marine Environment Monitoring Service (CMEMS) and is forced by ERA Interim reanalysis and assimilates (every week) observations from different platforms. The detailed setup and performance of the TOPAZ4 reanalysis, including the counts of observations and the temporal variations of the data counts are described in Xie et al. (2017). Of particular relevance for GS are the assimilation of Argo profiles, research cruises CTDs from Institute of Oceanology Polish Academy of Science (IOPAS) and Alfred-Wegener Institute (AWI) (Sakov et al. 2012), satellite sea ice concentration, sea surface temperature and sea level anomaly from the CMEMS platforms.

2.3 Sea ice data:

Monthly mean sea ice concentrations (SIC) from Nimbus-7 SMMR and DMSP SSM/I-SSMIS Passive Microwave Data, Version 1 (Cavalieri et al. 1996) were obtained from the National Snow and Ice Data Centre for the period 1991–2017. The dataset provides a continuous time series of SIC on a polar projection at a grid scale size of 25km by 25km. Sea ice velocity data was taken from the Polar Pathfinder Daily 25 km EASE-Grid Sea Ice Motion Vectors (Tschudi et al. 2019).

2.4 Methods and Evaluation of TOPAZ4

We estimated the strength of the GSG circulation by area-averaging the winter-mean (DJF) barotropic stream function anomalies within the 3000m isobath in the region 73 N:78 N; 12 W:9 E (as marked with green box in Fig. 1b). The area-averaged values were then standardized over the complete time period 1991–2017 to estimate the ‘gyre index’ (Fig. 1c). In this study we focused only on the winter (DJF) season as the local sea ice in GS can only form during winter and also the strength of the GSG circulation peaks during winter (Fig. 1c). Composite analysis of DJF mean potential temperature anomaly was performed by averaging the same for strong and weak gyre index years which were determined when the gyre

123 index crosses the 0.75 and -0.75 mark respectively. The 0.75 threshold was chosen to consider only the sufficiently
124 strong/weak gyre circulation periods. Throughout the article, all regression and correlation analysis were performed with the
125 detrended time series for the corresponding variables. Freshwater content was calculated using the following formula

$$\int_{z}^{surf} \frac{S_{ref} - S}{S_{ref}} \, dz$$

126 where, S is salinity and the reference salinity S_{ref} is chosen as 34.8 psu.
127
128 The standard deviation of winter-mean DJF SIC, in both observation and TOPAZ4, showed high variability along the MIZ in
129 western GS and the Odden region in central GS (Fig. 2). Note that, the TOPAZ4 reanalysis data exhibits a more confined
130 MIZ than observations, which is a known model deficiency (Sakov et al. 2012). The sea ice model (Hunke and Dukowicz,
131 1997), used in TOPAZ4, has a narrower transition zone between the pack ice and the open ocean. Although assimilation of
132 the sea ice observations does slightly improve the position of MIZ in TOPAZ4 compared to observation, the sharp transition
133 in a narrow band still remains, which could have resulted in higher standard deviations in a narrow MIZ of TOPAZ4 as
134 observed in Fig. 2b. However, as we will find in the next section, the sea ice response to the atmospheric and oceanic
135 processes explained in the study can be significantly found in both the observation and TOPAZ4 with slightly higher signals
136 along the MIZ in TOPAZ4. Thus the higher signal-to-noise ratio in TOPAZ4 should not affect the qualitative aspects of the
137 processes and their influence on SIC, which is the main objective of the study.

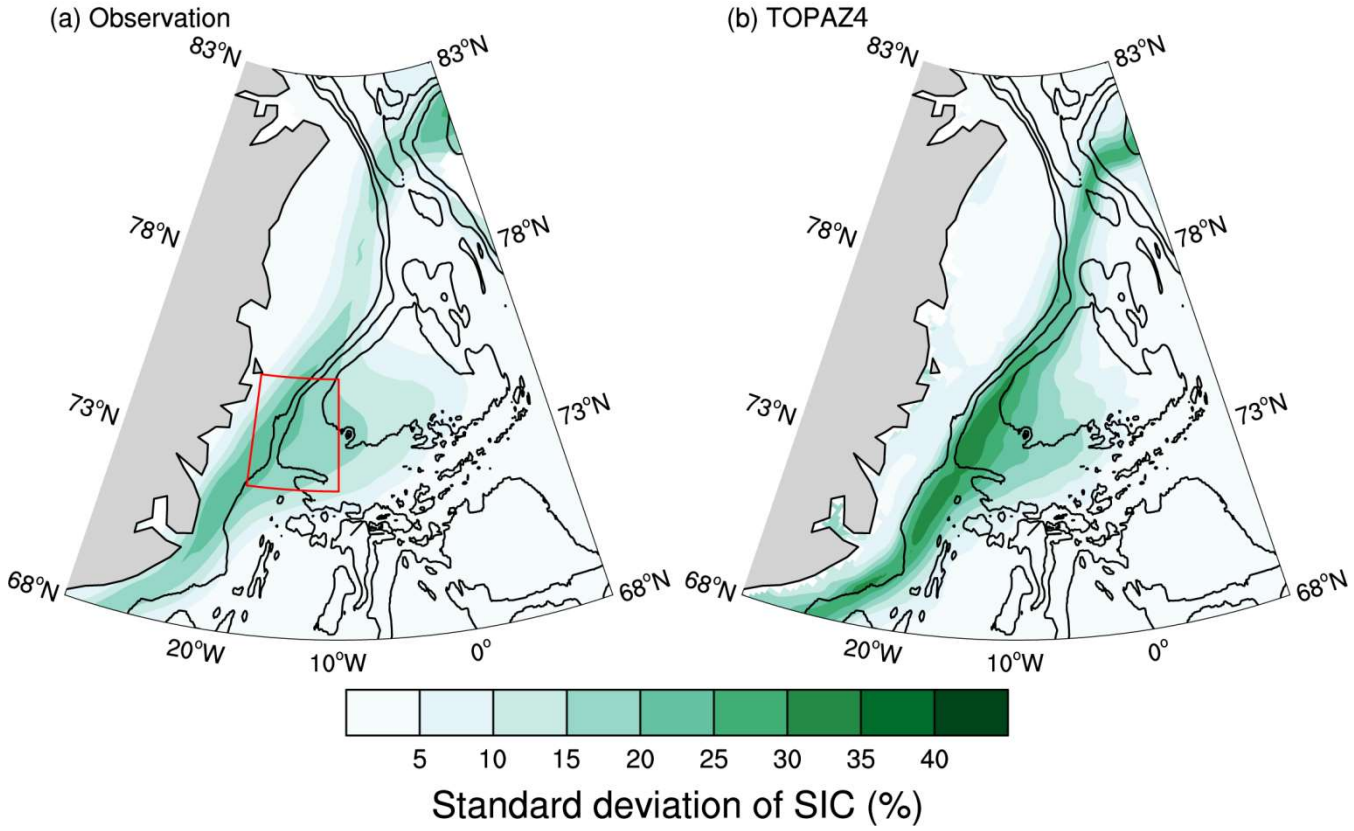

Figure 2: Standard deviations of DJF mean sea ice concentration for the period 1991–2017 from (a) satellite observations (b) TOPAZ4 reanalysis. The red box with high values is drawn over the region 72N:75N; 18W:10W and is referred to as western GS hereafter.

For evaluation of the oceanic conditions in TOPAZ4 we used temperature and salinity observations obtained from EN4 (version 4.2.1) quality controlled analyses with Levitus et al. (2009) corrections applied. Here we chose to compare the oceanic parameters in a region (as marked in Fig. 2) in western GS where the standard deviation of the SIC is found to be maximum both in TOPAZ4 and observations. Also we will show in the next section that SIC response to the processes described here is most profound in this region. Hereafter we refer to this region as western GS for simplicity. Fig. 3 shows the spatio-temporal patterns of sea surface temperature (SST) and salinity (SSS) in western GS as found in TOPAZ4 and EN4. Although the temporal evolution of these parameters are well captured in TOPAZ4, compared to observation, the westward extension of the warm and saline waters was found to be less in TOPAZ4. This indicates that the front between the cold and fresh waters along the Greenland shelf and the warm and saline waters in the western GS is slightly shifted towards the east in TOPAZ4 compared to observation. This could be a reason for the fact that higher standard deviation of SIC is

found slightly toward the east in TOPAZ4 than observations (Fig. 2). In western GS, both the surface and subsurface temperature in TOPAZ4 was found to be colder compared to observations (Fig. 4). The negative biases in TOPAZ4 were more profound in the subsurface for both temperature and salinity. Xie et al., (2017) also found a similar result with TOPAZ4 and attributed it to sparse observations. Using the potential density difference between 200m and the surface as an indicator of the stratification, we found that TOPAZ4 has weaker stratification compared to observations (Fig. 4e). Consistent with the cold bias in TOPAZ4, winter-mean SIC in TOPAZ4 is higher than the satellite observation in the western GS (Fig. 4f). However, we found a strong correlation (r=0.9) between the SIC in observation and TOPAZ4. This indicates that the interannual variability of SIC, which is the focus of the study, is quite consistent in both TOPAZ4 and observation.

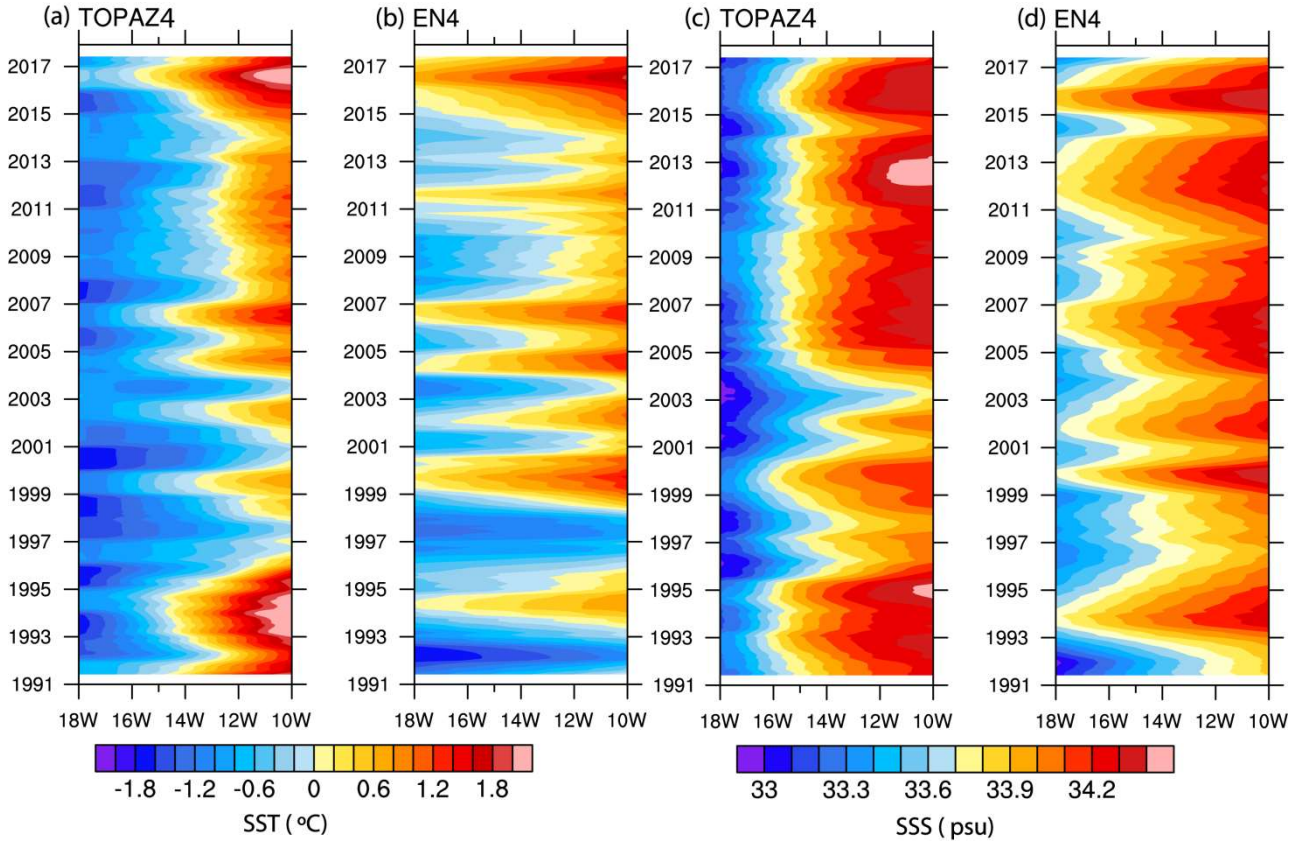

Figure 3: Hovmoller (longitude-time) diagram of the SST (^{o}C; a,b) and SSS (psu; c,d) over the region over 72 N:75 N; 18 W:10 W in the western GS as marked in Fig. 2. (a) and (c) are for TOPAZ4 and (b) and (d) for EN4 observations. In all cases data were smoothed with one year running mean.

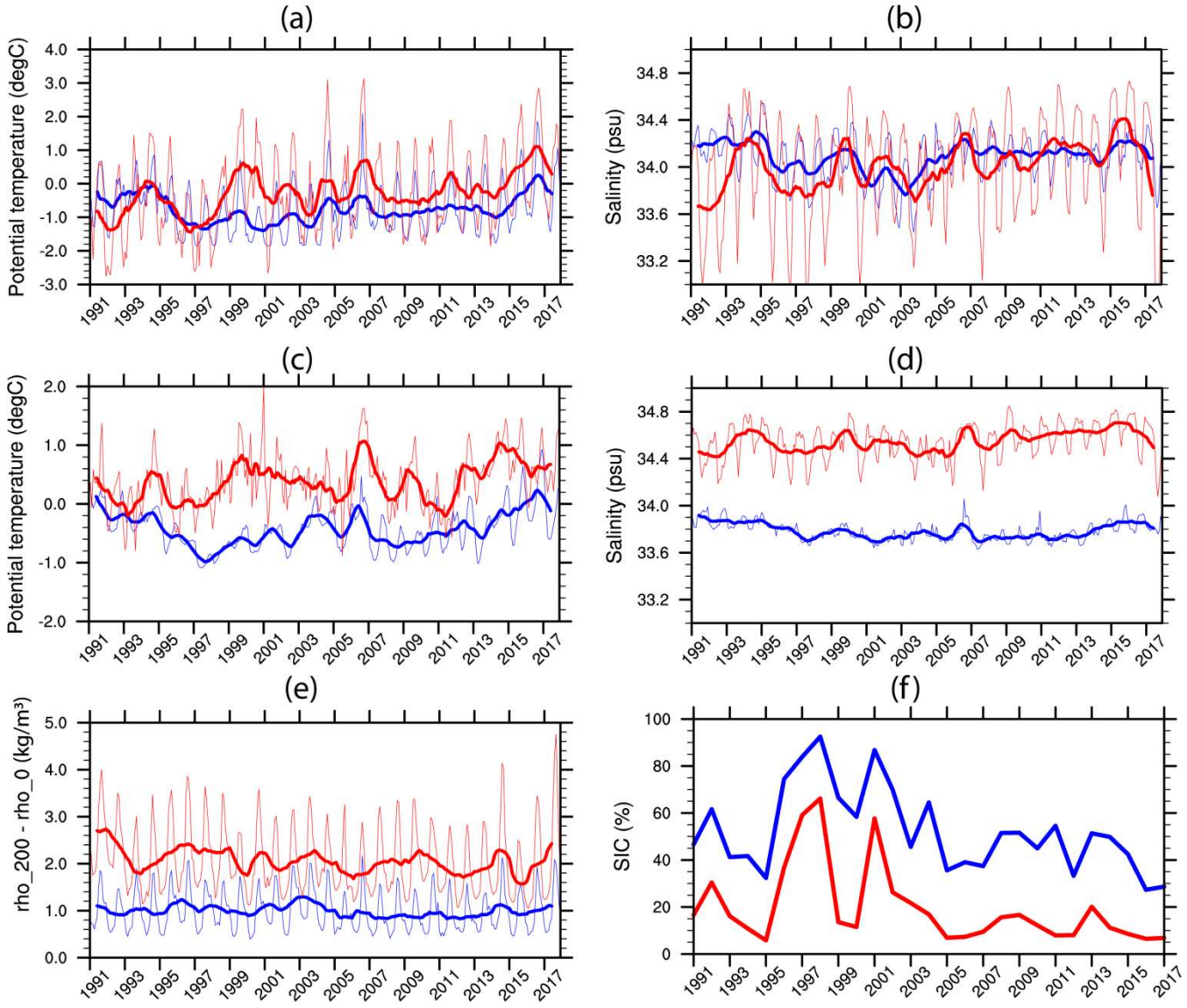

Figure 4: Comparison between EN4 observation (red lines) and TOPAZ4 (blue lines). Monthly mean (thin lines) and one year running mean (thick lines) of potential temperature (a,c), salinity (b,d) and stratification index (e, difference of potential density between 200m and surface) averaged over 72 N:75 N; 18 W:10 W in the western GS as marked in Fig. 2. (a,b) are for 0-50m depth average and (c,d) for 100-400m depth average. (f) DJF mean sea ice concentration in the same region from satellite observation (red) and TOPAZ4 (blue).

3. Results

The regression map of winter mean SIC on the gyre index showed significant negative SIC in the western GS (Fig. 5). The spatial pattern of the regression coefficients closely resembles the standard deviation of winter mean SIC in the GS, as shown in Fig. 2. This indicates that a considerable amount of the SIC variability in GS can be associated with GSG circulation. However, it should be noted that the atmospheric forcing in the NS can influence both the GSG circulation (Aagaard 1970; Legutke 2002; Chatterjee et al. 2018) and SIC variability in the GS (Germe et al. 2011).

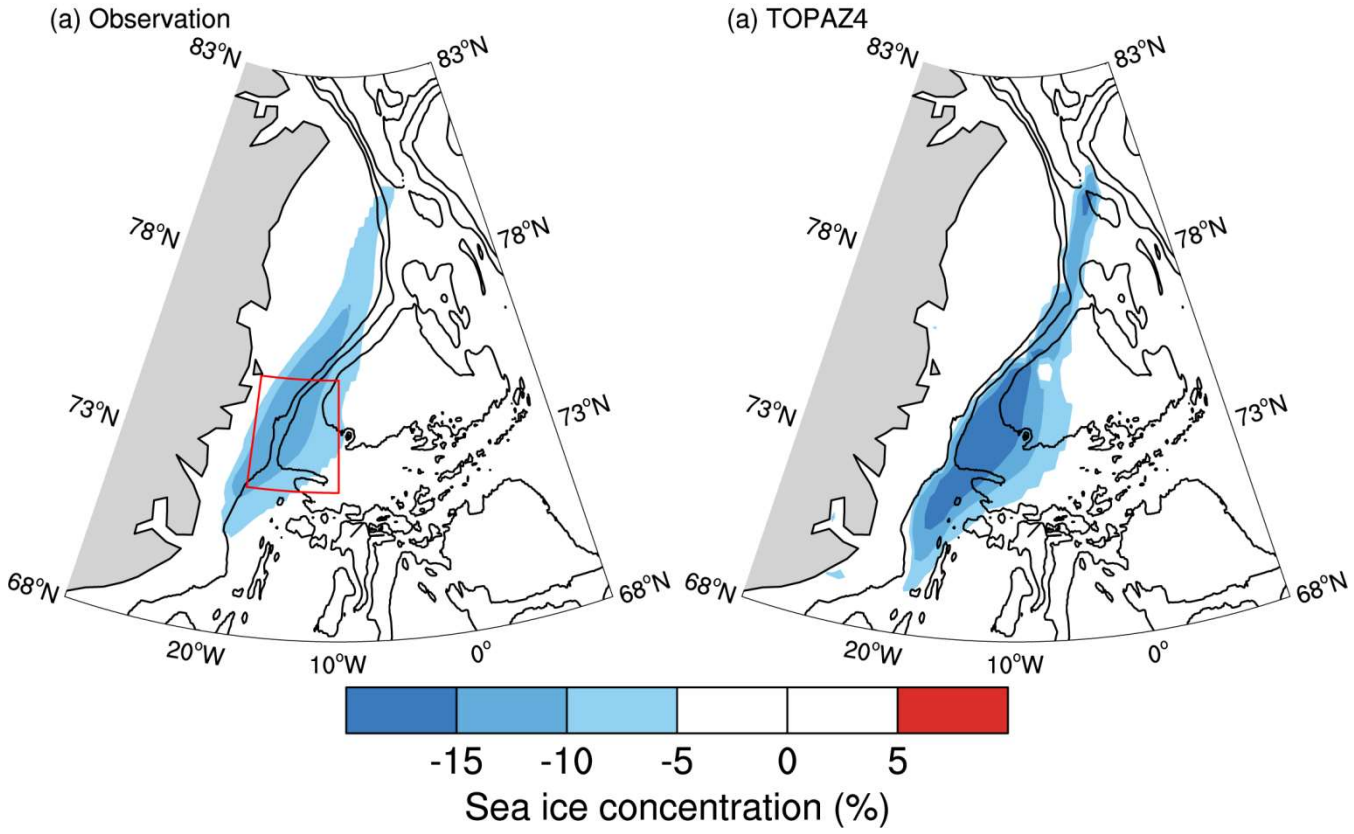

Figure 5: Linear regression of winter mean (DJF) sea ice concentration from (a) satellite observation (b) TOPAZ reanalysis on the gyre index. Only significant values at 95 % level are shown. Contours are bottom topography drawn at every 1000 m.

To elucidate the possible influence of atmospheric circulation pattern associated with GSG circulation on the SIC variability in the GS, linear regression of the sea level pressure anomalies on the gyre index was calculated and shown in Fig. 6. The large-scale atmospheric circulation shows a positive NAO-like pattern associated with a strong GSG circulation, but with centres of actions north of their usual locations (Fig. 6). The GSG circulation responds to the anomalous wind stress curl induced by the low SLP anomaly patterns in the NS (Chatterjee et al. 2018). However, we found that the station based NAO index, with its spatial feature highlighting the Icelandic low and Azores high, (https://climatedataguide.ucar.edu/sites/default/files/nao_station_seasonal.txt) and the gyre index have a very low correlation (r = 0.2). This further points to the importance of the spatial variability of NAO (Zhang et al. 2008; Moore et al. 2012) and its influence on the Nordic Seas circulation. Also note that the low correlation could be due to the fact that the equatorward pole of NAO doesn't exhibit much significant regression patterns in Fig. 6.

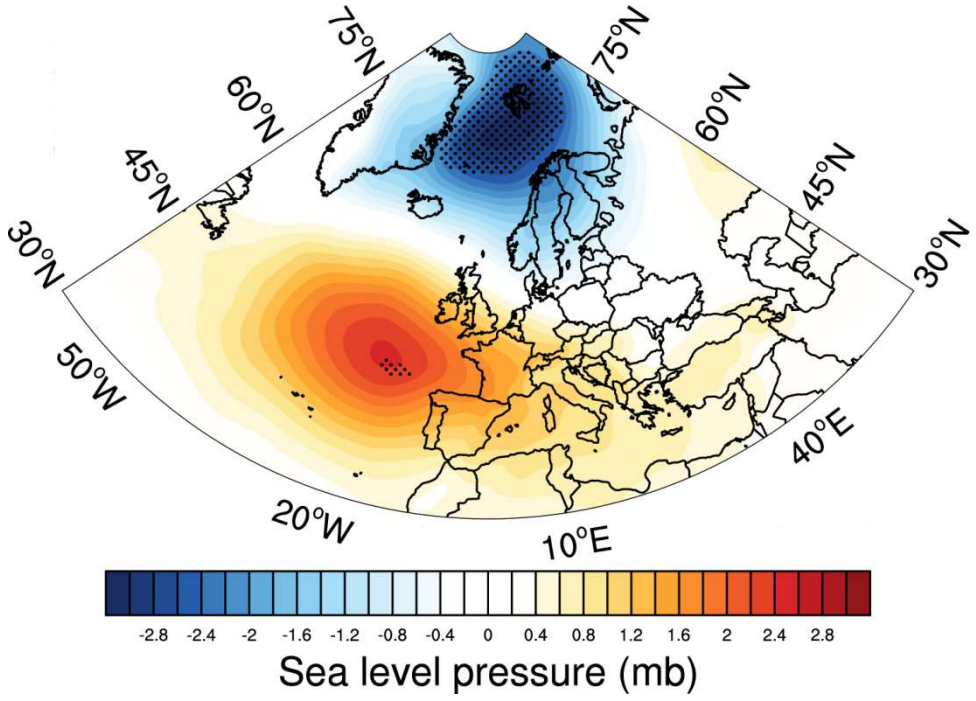

Figure 6: Linear regression of DJF mean sea level pressure anomaly on the gyre index. Regions with 95% statistical significance are dotted.

The mean southward sea ice export in the GS across the FS (Fig 7a) is strongly driven by the geostrophic winds in this region (Smedsrud et al. 2017). The low SLP pattern over NS associated with the GSG circulation can induce anomalous northerlies in GS. Linear regression of sea ice velocities on the gyre index showed anomalous northward sea ice velocities in GS associated with increase in GSG strength (Fig. 7b). This indicates that the anomalous northerly winds during a strong GSG circulation would lead to Ekman drift of sea ice which tends to push the sea ice towards the Greenland coast and reduce

the mean southward sea ice velocities in this region (Fig. 7a). This could lead to reduced sea ice export in this region and result in low SIC.

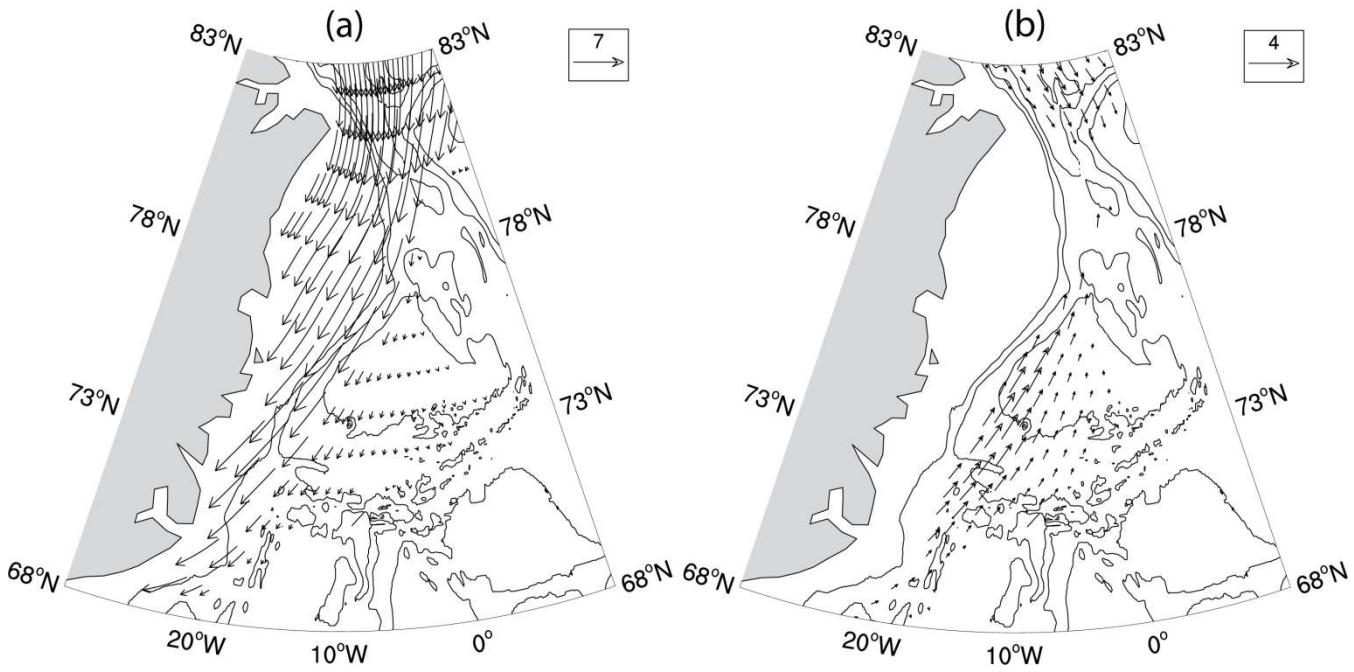

Figure 7: (a) Climatological (1991–2017) DJF sea ice velocity vectors (cm/s) from satellite observations. (b) Regression of DJF sea ice velocity anomalies (cm/s) on the gyre index. Only results significant at 95 % are shown for clarity. Contours are bottom topography drawn at every 1000 m.

Next, we investigate GSG's potential in influencing the oceanic conditions and hence the sea ice in the GS, given that the local oceanic conditions largely affect the sea ice conditions therein (Johannessen et al. 1987; Visbeck et al. 1995; Kern et al. 2010; Selyuzhenok et al. 2020). Figure 8a shows the difference in ocean temperature anomaly in the upper 400m averaged for the strong and weak GSG circulation years (marked in Fig 8b; see methods for definitions). The average temperature anomaly for the strong GSG circulation years was found to be ~1^{o}C higher than the same during weak GSG circulation years. The warm anomalies further extend eastward with the JMC towards the central GS and could potentially affect the sea ice formation in the Odden region. Further, we found significant positive correlation ($r=0.7$, $p<0.01$; Fig 8b) between gyre index and temperature advection (in upper 400m) in the western GS (marked region in Fig. 8a), where maximum GSG influence on SIC is found (Fig. 3a). This suggests that a strong GSG circulation recirculates the warm AW anomalies into the western GS from the FS. This is consistent with earlier study indicating an increased oceanic heat content in the western GS due to a stronger GSG circulation (Chatterjee et al., 2018).

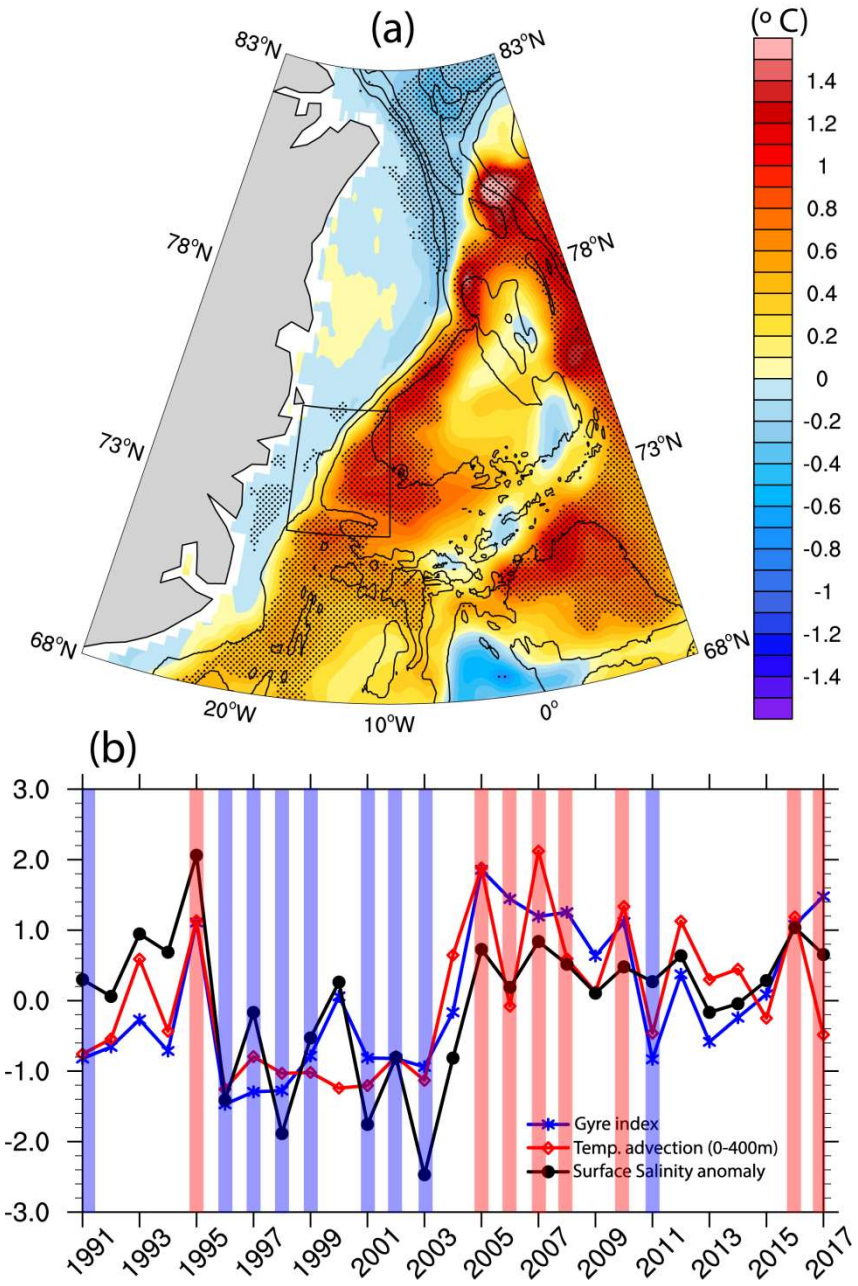

Figure 8: (a) Difference between 400 m depth averaged potential temperature anomalies (^{o}C) averaged for strong (red bars in (b)) and weak (blue bars in (b)) gyre index years. (b) Gyre index (blue), and standardized surface salinity anomaly (black), temperature advection ($U.\nabla T$) in upper 400 m (red) for DJF over the region 72 N: 75 N; 18 W : 10 W, as marked in (a).

However, it should be noted that the recirculated AW in the GS still remains dense enough to be in subsurface (Schlichtholz & Houssais 1999; Eldevik et al. 2009) and needs to be vertically mixed to have an impact on the sea ice. We found that the upper ocean stratification in the western GS strongly covaries with GSG circulation strength (Fig. 9a). The analysis shows that a weakening of the stratification in the upper part of the water column coincides with a stronger GSG circulation and vice versa (Fig. 9a). Further, warm and saline signatures in the upper ocean can be found during strong GSG circulation, indicating enhanced vertical mixing of the AW in the western GS (Figs. 9b,c). This is further confirmed by significant positive correlation ($r=0.7$, $p<0.01$) between surface salinity anomaly and gyre index (Fig. 8b). These surface anomalies can further inhibit new sea ice formation and also may cause melting of existing sea ice from the bottom.

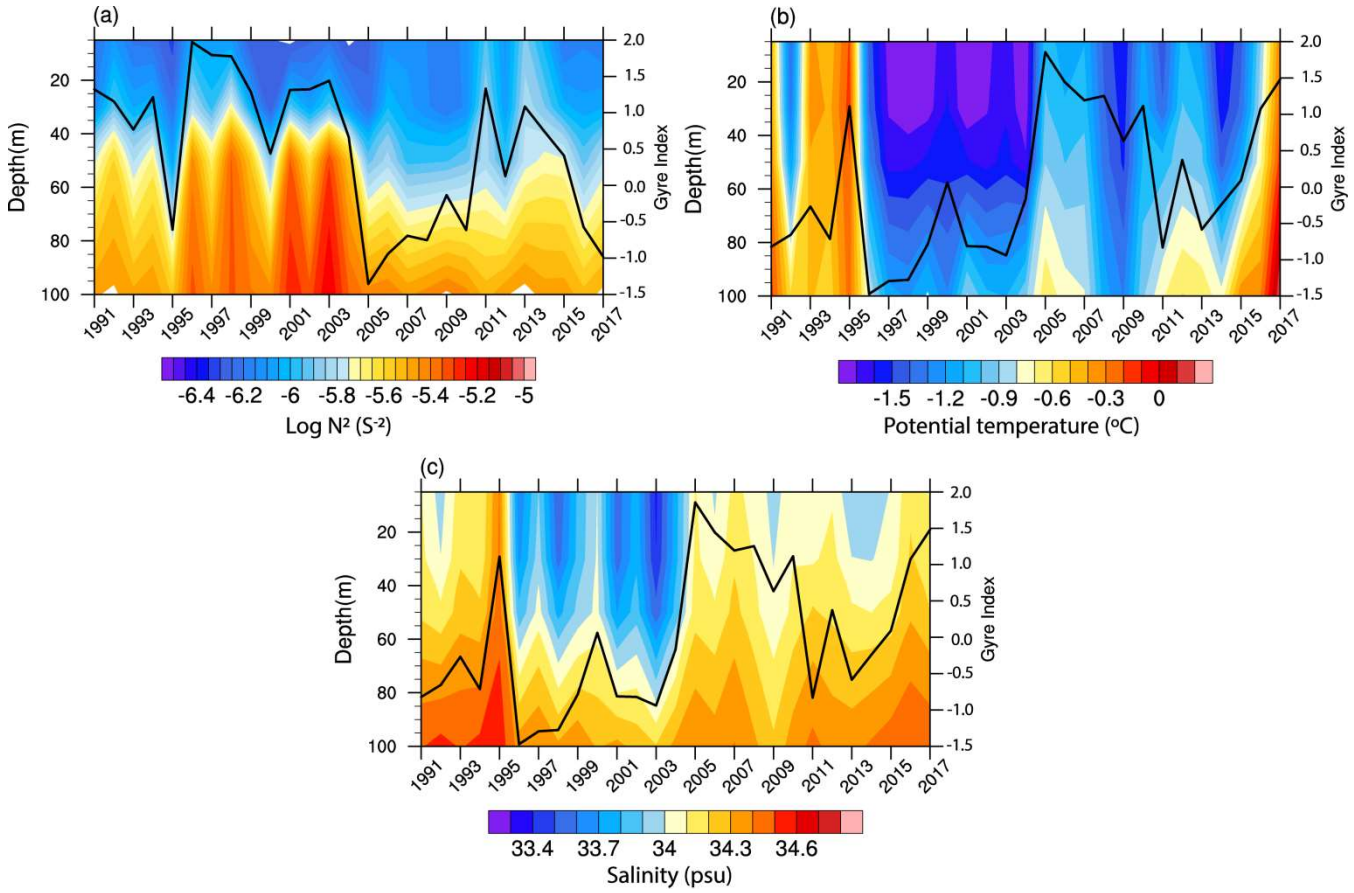

Figure 9: (a) Logarithm of squared Brunt-Väisälä Frequency (N^2, colour shaded) (b) potential temperature (c) salinity for DJF over the region 72 N:75 N; 18 W:10 W, as marked in Figure 8a. The black timeseries against the right Y axis is the gyre index in all three panels. Note that the gyre index is plotted against a reversed Y axis in (a) for ease of comparison.

241

242 **4. Discussions and Conclusions**

243 Here we investigated the combined influence of atmospheric and oceanic circulations on the interannual variability of the
244 winter mean SIC variability in the GS and showed that NS, in particular the GSG circulation can significantly contribute to
245 the SIC variability in western GS. Fig. 10 shows the flow chart and a schematic illustration of the mechanisms proposed in
246 this study. The large-scale atmospheric circulation pattern that influences the GSG circulation resembles a NAO-like pattern
247 with its northern centre of action situated northeast of the typical NAO pattern. The cyclonic GSG circulation strengthens in
248 response to the positive wind stress curl induced by the low SLP anomaly in the NS (Legutke 2002, Chatterjee et al. 2018).
249 The resulting northerly wind anomalies over GS can potentially alter the sea ice export across the FS (Kwok & Rothrock
250 1999; Jung & Hilmer 2001; Vinje 2001; Tsukernik et al. 2010; Smedsrud et al. 2011; Ionita et al. 2016). However, winter
251 mean SIC in the GS and FS ice area flux are not strongly correlated (Kwok et al., 2004; Germe et al., 2011), suggesting that
252 the SIC variability in the GS can be significantly influenced by the local sea ice dynamics and oceanic conditions.

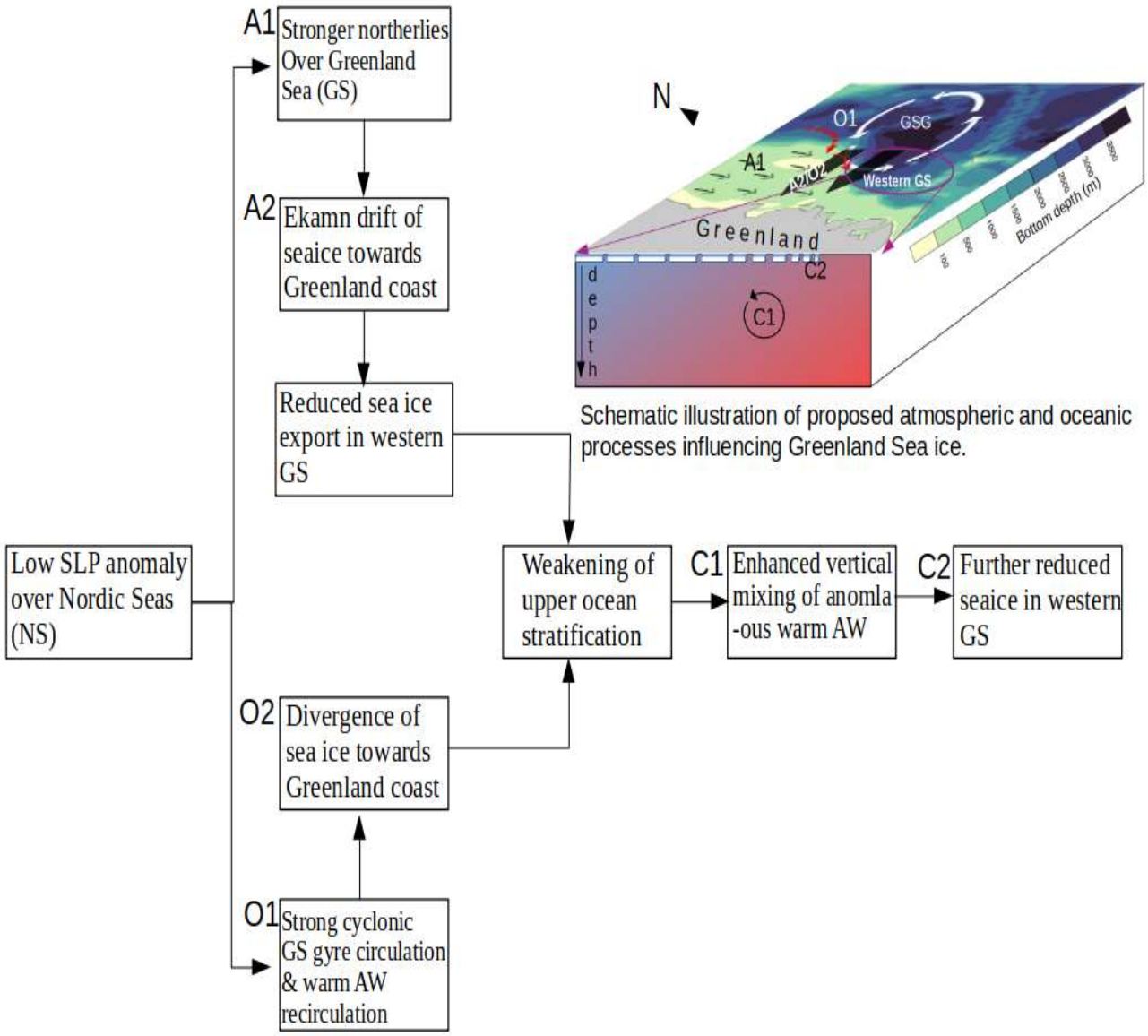

Figure 10: A flow chart and schematic diagram of the proposed processes influencing the SIC variability in the western GS.

Anomalous winds in the Nordic Seas are known to influence the SIC in the GS through Ekman drift of the sea ice (Germe et al., 2011). During time-periods with anomalously low SLP over NS, anomalous northerly winds and associated Ekman drift towards the Greenland coast that can reduce the sea ice export in the western and central GS (Fig 8b). Enhanced Ekman divergence due to a strengthened GSG circulation can further lead to reduced freshwater and sea ice in the western GS (Fig. 11). We found that these can lead to weakening of the upper ocean stratification in the western GS (Fig. 9a). At the same time, a stronger GSG circulation recirculates the warm and saline subsurface AW anomalies from the FS into the western GS (Fig 8a). These AW anomalies can warm the surface waters by enhanced vertical mixing in a weakly stratified condition (Fig. 9) and can cause further reduction of SIC by inhibiting new sea ice formation or even melting the sea ice from bottom. Although our study doesn't show bottom melting of the sea ice, this can be realized from the findings by Ivanova et al. (2011) which showed enhanced bottom melting in this region during positive NAO periods. Thus, the SIC variability in the western GS responds to simultaneous influences from the atmospheric and oceanic circulation (Fig. 10). Despite the known influences of smaller scale processes, such as eddies and wave interactions on the SIC in the western GS, our results show that the larger scale processes can also significantly affect the SIC variability in the region, particularly on interannual timescales when the impacts of smaller scale processes can cancel out or may not be strong enough to dampen the impact of larger scale processes. However, as found in Raj et al., (2020) interactions between the gyre circulation and the eddies can be an important factor controlling the oceanic conditions and hence the SIC in the western GS.

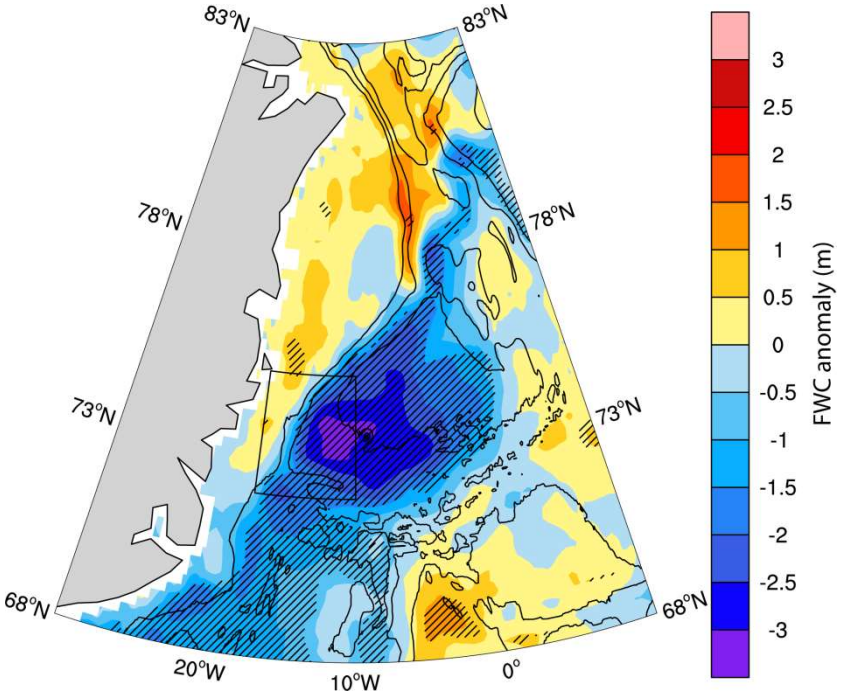

Figure 11: Difference in freshwater content (FWC) anomaly (m) between strong and weak gyre index periods. Significant differences at 95% level are stippled.

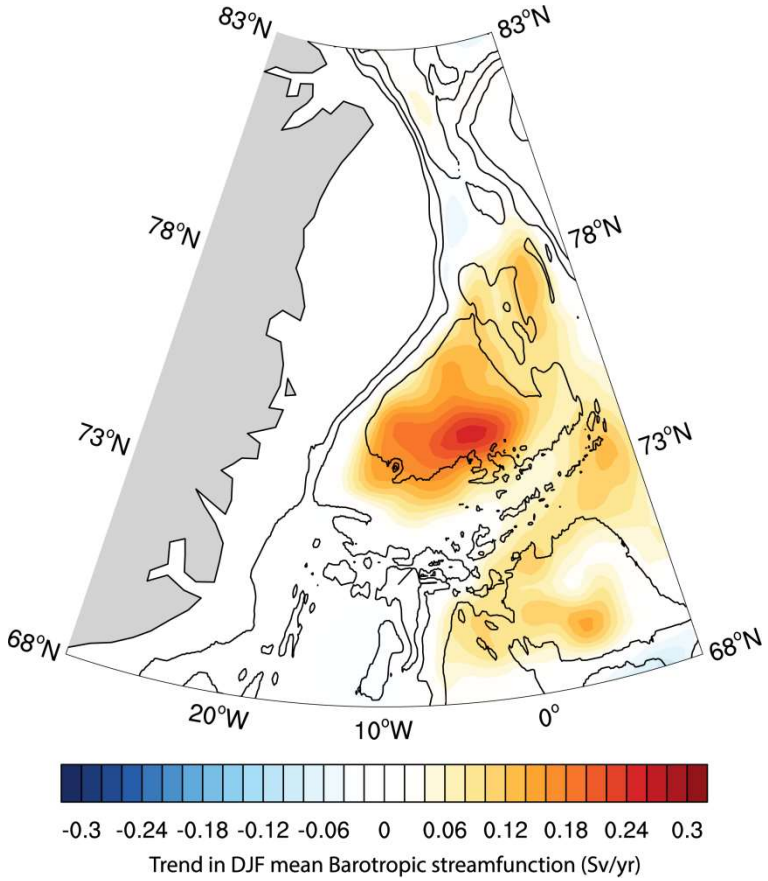

Figure 12: Linear trend (Sv/year) in winter mean (DJF) barotropic stream function for 1991–2017. Only significant values at 95 % level are shown for clarity. Contours are bottom topography drawn at every 1000 m.

SIC in the GS is an important component of the regional and global climate (Moore et al. 2015; Kopec et al. 2016; Dall'Osto et al. 2018). It is thus important to understand the driving mechanisms for the variability of it. This study finds one of those mechanisms highlighting the role of large scale atmospheric and oceanic circulations in the NS. Observations and modelling results suggest stronger atmospheric forcing in the NS due to spatial variation of the NAO (Zhang et al. 2008) and its tendency towards positive phase in a warmer climate (Bader et al. 2011; Stephenson et al. 2016). Consistent with that we find a significant positive trend in the GSG circulation strength during the study period (Fig. 12). The response of GSG circulation to this altered atmospheric forcing can further be realized with increased GSG strength (Fig. 1c) and a sudden northeastward displacement of NAO's poleward centre of action in the Nordic Seas during early 2000s (Fig. 1a in Zhang et al., 2008). Recent observations suggest intensified convection in the GSG and resulting changes in water mass formation during the last two decades (Lauvset et al., 2018; Brakstad et al., 2019). Lauvset et al., (2018) further discussed the role of

recirculated AW on inducing intensified convection in the GSG through surface salinity anomaly. Consistent with this, our results show that the salinity anomalies and intensified convection in the GSG can be induced by a stronger GSG circulation (in response to the atmospheric forcing) which helps in recirculation of AW anomalies in the GS. Thus we propose that the atmospheric forcing over the NS imposes a positive oceanic feedback (Fig. 13). The low SLP anomaly over the NS strengthens the GSG circulation. The Ekman divergence pushes the freshwater and sea ice from the GS interior towards the coast. Enhanced AW recirculation due to a stronger GSG and weakened stratification due to reduced freshwater allows the warm and saline AW anomalies to get vertically mixed and increase the temperature and salinity in the central GS. The increased salinity further helps in a stronger GSG circulation, completing the feedback loop. The findings of the study thus highlight that interaction between large scale atmospheric and oceanic circulation in NS is crucial for understanding the North Atlantic and Arctic oceanic connections.

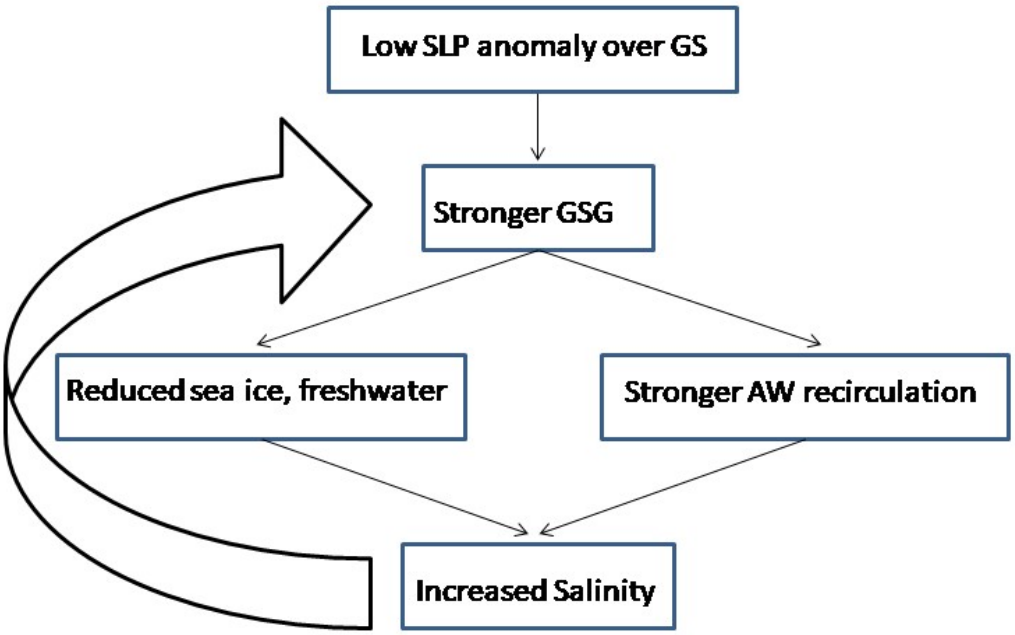

Figure 13: A proposed positive oceanic feedback induced by atmospheric forcing in NS.

Acknowledgments

Sea ice concentration (https://nsidc.org/data/NSIDC-0051/versions/1) and velocity (https://nsidc.org/data/nsidc-0116/versions/4) are obtained from the National Snow and Ice Data Centre. The TOPAZ4 simulations have used grants of computing time (nn2993k) and storage (ns2993k) from the Sigma2 infrastructure. The monthly TOPAZ4 results used in this study are obtained via CMEMS (marine.copernicus.eu). EN4 (version 4.2.1) observational data is provided by UK Met Office Hadley Centre and obtained from https://www.metoffice.gov.uk/hadobs/en4/download-en4-2-1.html. Authors thank Ola M Johannessen, Nansen Scientific Society and Jiping Xie, NERSC for valuable suggestions and help with TOPAZ4 data during the course of the study. All figures were made using The NCAR Command Language (Version 6.4.0).

Declarations

Funding (information that explains whether and by whom the research was supported)

Not Applicable

Conflicts of interest/Competing interests (include appropriate disclosures)

Authors declare no Conflicts of interest/Competing interests

Availability of data and material (data transparency)

All the data used here are freely available on respective data portals (links provided in the 'Acknowledgements' section)

Code availability (software application or custom code)

All the codes are available on reasonable request to the corresponding author.

Authors' contributions

SC conceived the idea in discussion with RPR and wrote the manuscript. SC performed all the analyses. All authors contributed in improvement and writing of the manuscript.

References

Aagaard, K.: Wind-driven transports in the Greenland and Norwegian seas, Deep. Res. Oceanogr. Abstr., doi:10.1016/0011-7471(70)90021-5, 1970.

Aagaard, K. and Carmack, E. C.: The role of sea ice and other fresh water in the Arctic circulation, J. Geophys. Res., doi:10.1029/jc094ic10p14485, 1989.

Bader, J., Mesquita, M. D. S., Hodges, K. I., Keenlyside, N., Østerhus, S. and Miles, M.: A review on Northern Hemisphere sea-ice, storminess and the North Atlantic Oscillation: Observations and projected changes, Atmos. Res., doi:10.1016/j.atmosres.2011.04.007, 2011.

Belkin, I. M., Levitus, S., Antonov, J. and Malmberg, S. A.: "Great Salinity Anomalies" in the North Atlantic, Prog. Oceanogr., doi:10.1016/S0079-6611(98)00015-9, 1998.

Bourke, R. H., Paquette, R. G. and Blythe, R. F.: The Jan Mayen Current of the Greenland Sea, J. Geophys. Res., doi:10.1029/92jc00150, 1992.

Brakstad, A., K. Våge, L. Håvik, and G. W. K. Moore, 2019: Water Mass Transformation in the Greenland Sea during the Period 1986–2016. J. Phys. Oceanogr., 49, 121–140, https://doi.org/10.1175/JPO-D-17-0273.1.

Buckley, M. W. and Marshall, J.: Observations, inferences, and mechanisms of the Atlantic Meridional Overturning Circulation: A review, Rev. Geophys., doi:10.1002/2015RG000493, 2016.

Campbell, W. J., Gloersen, P., Josberger, E. G., Johannessen, O. M., Guest, P. S., Mognard, N., Shuchman, R., Burns, B. A., Lannelongue, N. and Davidson, K. L.: Variations of mesoscale and large-scale sea ice morphology in the 1984 marginal ice zone experiment as observed by microwave remote sensing, J. Geophys. Res. Ocean., doi:10.1029/JC092iC07p06805, 1987.

Cavalieri, D.J., Parkinson, C. L., Gloersen, P. & Zwally H. J.: Sea Ice Concentrations From Nimbus-7 SMMR and DMSP SSM/I Passive Microwave Data, Natl. Snow and Ice Data Cent., Boulder, Colorado, 1996 [Updated 2018].

Chatterjee, S., Raj, R. P., Bertino, L., Skagseth, Ravichandran, M. and Johannessen, O. M.: Role of Greenland Sea Gyre Circulation on Atlantic Water Temperature Variability in the Fram Strait, Geophys. Res. Lett., doi:10.1029/2018GL079174, 2018.

Comiso, J. C., Wadhams, P., Pedersen, L. T. and Gersten, R. A.: Seasonal and interannual variability of the Odden ice tongue and a study of environmental effects, J. Geophys. Res. Ocean., doi:10.1029/2000jc000204, 2001.

Dall'Osto, M., Geels, C., Beddows, D. C. S., Boertmann, D., Lange, R., Nøjgaard, J. K., Harrison, R. M., Simo, R., Skov, H. and Massling, A.: Regions of open water and melting sea ice drive new particle formation in North East Greenland, Sci. Rep., doi:10.1038/s41598-018-24426-8, 2018.

Dee, D. P., Uppala, S. M., Simmons, A. J., Berrisford, P., Poli, P., Kobayashi, S., Andrae, U., Balmaseda, M. A., Balsamo, G., Bauer, P., Bechtold, P., Beljaars, A. C. M., van de Berg, L., Bidlot, J., Bormann, N., Delsol, C., Dragani, R., Fuentes, M., Geer, A. J., Haimberger, L., Healy, S. B., Hersbach, H., Hólm, E. V., Isaksen, L., Kållberg, P., Köhler, M., Matricardi, M., Mcnally, A. P., Monge-Sanz, B. M., Morcrette, J. J., Park, B. K., Peubey, C., de Rosnay, P., Tavolato, C., Thépaut, J. N. and

Vitart, F.: The ERA-Interim reanalysis: Configuration and performance of the data assimilation system, Q. J. R. Meteorol. Soc., doi:10.1002/qj.828, 2011.

Deser, C., Walsh, J. E. and Timlin, M. S.: Arctic sea ice variability in the context of recent atmospheric circulation trends, J. Clim., doi:10.1175/1520-0442(2000)013<0617:ASIVIT>2.0.CO;2, 2000.

Dickson, R. R., Meincke, J., Malmberg, S. A. and Lee, A. J.: The "great salinity anomaly" in the Northern North Atlantic 1968-1982, Prog. Oceanogr., doi:10.1016/0079-6611(88)90049-3, 1988.

Eldevik, T. and Nilsen, J. E. Ø.: The arctic-atlantic thermohaline circulation, J. Clim., doi:10.1175/JCLI-D-13-00305.1, 2013.

Eldevik, T., Nilsen, J. E., Iovino, D., Anders Olsson, K., Sandø, A. B. and Drange, H.: Observed sources and variability of Nordic seasoverflow, Nat. Geosci., doi:10.1038/ngeo518, 2009.

Germe, A., Houssais, M. N., Herbaut, C. and Cassou, C.: Greenland Sea sea ice variability over 1979-2007 and its link to the surface atmosphere, J. Geophys. Res. Ocean., 116(10), 1–14, doi:10.1029/2011JC006960, 2011.

Grebmeier, J. M., Smith, W. O. and Conover, R. J.: Biological processes on Arctic continental shelves: Ice-ocean-biotic interactions., 2011.

Hattermann, T., Isachsen, P. E., Von Appen, W. J., Albretsen, J. and Sundfjord, A.: Eddy-driven recirculation of Atlantic Water in Fram Strait, Geophys. Res. Lett., doi:10.1002/2016GL068323, 2016.

Hilmer, M. and Jung, T.: Evidence for a recent change in the link between the North Atlantic Oscillation and Arctic sea ice export, Geophys. Res. Lett., doi:10.1029/1999GL010944, 2000.

Hunke, E. C. and Dukowicz, J. K.: An elastic-viscous-plastic model for sea ice dynamics, J. Phys. Oceanogr., 27, 1849–1867, 1997.

Hurrell, J. W.: Decadal trends in the North Atlantic oscillation: Regional temperatures and precipitation, Science (80-.)., doi:10.1126/science.269.5224.676, 1995.

Instanes, A., Anisimov, O., Brigham, L., Goering, D., Khrustalev, L. N., Ladanyi, B., Larsen, J. O., Smith, O., Stevermer, A., Weatherhead, B. and Weller, G.: Infrastructure: buildings, support systems, and industrial facilities, in Arctic Climate Impact Assessment., 2005.

Ionita, M., Scholz, P., Lohmann, G., Dima, M. and Prange, M.: Linkages between atmospheric blocking, sea ice export through Fram Strait and the Atlantic Meridional Overturning Circulation, Sci. Rep., doi:10.1038/srep32881, 2016.

Jeansson, E., Olsen, A. and Jutterström, S.: Arctic Intermediate Water in the Nordic Seas, 1991–2009, Deep. Res. Part I Oceanogr. Res. Pap., doi:10.1016/j.dsr.2017.08.013, 2017.

Johannessen, O. M., Johannessen, J. A., Svendsen, E., Shuchman, R. A., Campbell, W. J. and Josberger, E.: Ice-edge eddies in the Fram Strait marginal ice zone, Science (80-.)., doi:10.1126/science.236.4800.427, 1987.

Johannessen, O. M., Bengtsson, L., Miles, M. W., Kuzmina, S. I., Semenov, V. A., Alekseev, G. V., Nagurnyi, A. P., Zakharov, V. F., Bobylev, L. P., Pettersson, L. H., Hasselmann, K. and Cattle, H. P.: Arctic climate change: Observed and modelled temperature and sea-ice variability, Tellus, Ser. A Dyn. Meteorol. Oceanogr., doi:10.1111/j.1600-0870.2004.00060.x, 2004.

Jung, T. and Hilmer, M.: The link between the North Atlantic oscillation and Arctic sea ice export through Fram Strait, J. Clim., doi:10.1175/1520-0442(2001)014<3932:TLBTNA>2.0.CO;2, 2001.

Kern, S., Kaleschke, L. and Spreen, G.: Climatology of the nordic (irminger, greenland, barents, kara and white/pechora) seas ice cover based on 85 GHz satellite microwave radiometry: 1992-2008, Tellus, Ser. A Dyn. Meteorol. Oceanogr., doi:10.1111/j.1600-0870.2010.00457.x, 2010.

Killworth, P. D.: On "Chimney" Formations in the Ocean, J. Phys. Oceanogr., doi:10.1175/1520-0485(1979)009<0531:ofito>2.0.co;2, 1979.

Kopec, B. G., Feng, X., Michel, F. A. and Posmentiera, E. S.: Influence of sea ice on Arctic precipitation, Proc. Natl. Acad. Sci. U. S. A., doi:10.1073/pnas.1504633113, 2016.

Kwok, R.: Fram Strait sea ice outflow, J. Geophys. Res., 109(C1), C01009, doi:10.1029/2003JC001785, 2004.

Kwok, R. and Rothrock, D. A.: Variability of Fram Strait ice flux temperature 2 , -7 % of the area of the Arctic Ocean . The winter area flux ranges from a minimum to a maximum of October May 1995 is 1745 km from a low of 1375 km the 1990 flux to a high of 2791 km The sea level pressu, J. Geophys. Res., 104(1998), 5177–5189, 1999.

Kwok, R., Cunningham, G. F., Wensnahan, M., Rigor, I., Zwally, H. J. and Yi, D.: Thinning and volume loss of the Arctic Ocean sea ice cover: 2003-2008, J. Geophys. Res. Ocean., doi:10.1029/2009JC005312, 2009.

Lauvset, S.K., Brakstad, A., Våge, K., Olsen, A., Jeansson, E., Mork, K.A.: Continued warming, salinification and oxygenation of the Greenland Sea gyre, Tellus A, 70 (1), pp.1-9, doi:10.1080/16000870.2018.1476434, 2018.

Legutke, S.: A Numerical Investigation of the Circulation In the Greenland and Norwegian Seas, J. Phys. Oceanogr., doi:10.1175/1520-0485(1991)021<0118:aniotc>2.0.co;2, 2002.

Levitus et al.: Global ocean heat content 1955-2008 in light of recently revealed instrumentation problems. Geophysical Research Letters, 36, L07608. doi:http://dx.doi.org/10.1029/2008GL037155, 2009

Lien, V. S., Hjøllo, S. S., Skogen, M. D., Svendsen, E., Wehde, H., Bertino, L., Counillon, F., Chevallier, M. and Garric, G.: An assessment of the added value from data assimilation on modelled Nordic Seas hydrography and ocean transports, Ocean Model., doi:10.1016/j.ocemod.2015.12.010, 2016.

Lind, S., Ingvaldsen, R. B. and Furevik, T.: Arctic warming hotspot in the northern Barents Sea linked to declining sea-ice import, Nat. Clim. Chang., doi:10.1038/s41558-018-0205-y, 2018.

Marshall, J. and Schott, F.: Open-ocean convection: Observations, theory, and models, Rev. Geophys., doi:10.1029/98RG02739, 1999.

Moore, G. W. K., Renfrew, I. A. and Pickart, R. S.: Multidecadal mobility of the north atlantic oscillation, J. Clim., doi:10.1175/JCLI-D-12-00023.1, 2013.

Moore, G. W. K., Vage, K., Pickart, R. S. and Renfrew, I. A.: Decreasing intensity of open-ocean convection in the Greenland and Iceland seas, Nat. Clim. Chang., doi:10.1038/nclimate2688, 2015.

Nansen, F.: Blant Sel og Bj•rn. Min forste Ishavs-Ferd [With Seals and Bears: My First Journey to the Arctic Seas], Jacob Dybwads Forlag, Oslo, 285 pp, 1924.

Raj, R. P., Chatterjee, S., Bertino, L., Turiel, A. & Portabella, M.: The Arctic Front and its variability in the Norwegian Sea, Ocean Sci., 15, 1729–1744, https://doi.org/10.5194/os-15-1729-2019, 2019.

Raj, R. P., Halo, I., Chatterjee, S., Belonenko, T., Bakhoday-Paskyabi, M., Bashmachnikov, I., Federov, A., Xie P. : Interaction between mesoscale eddies and the gyre circulation in the Lofoten Basin. *Journal of Geophysical Research: Oceans*, 125, e2020JC016102. https://doi.org/10.1029/2020JC016102, 2020.

Rogers, J. C., and Hung, M.-P. (2008), The Odden ice feature of the Greenland Sea and its association with atmospheric pressure, wind, and surface flux variability from reanalyses, Geophys. Res. Lett., 35, L08504, doi:10.1029/2007GL032938.

Sakov, P., Counillon, F., Bertino, L., Lister, K. A., Oke, P. R. and Korablev, A.: TOPAZ4: An ocean-sea ice data assimilation system for the North Atlantic and Arctic, Ocean Sci., doi:10.5194/os-8-633-2012, 2012.

Schott, F., Visbeck, M. and Fischer, J.: Observations of vertical currents and convection in the central Greenland Sea during the winter of 1988-1989, J. Geophys. Res., doi:10.1029/93jc00658, 1993.

Selyuzhenok, V., Bashmachnikov, I., Ricker, R., Vesman, A. & Bobylev, L.: Sea ice volume variability and water temperature in the Greenland Sea, The Cryosphere, 14, 477–495, https://doi.org/10.5194/tc-14-477-2020, 2020.

Serreze, M. C., Barrett, A. P., Slater, A. G., Woodgate, R. A., Aagaard, K., Lammers, R. B., Steele, M., Moritz, R., Meredith, M. and Lee, C. M.: The large-scale freshwater cycle of the Arctic, J. Geophys. Res. Ocean., doi:10.1029/2005JC003424, 2006.

Serreze, M. C., Holland, M. M. and Stroeve, J.: Perspectives on the Arctic's shrinking sea-ice cover, Science (80-.)., doi:10.1126/science.1139426, 2007.

Shuchman, R. A., Josberger, E. G., Russel, C. A., Fischer, K. W., Johannessen, O. M., Johannessen, J. and Gloersen, P.: Greenland Sea Odden sea ice feature: Intra-annual and interannual variability, J. Geophys. Res. Ocean., doi:10.1029/98jc00375, 1998.

Smedsrud, L. H., Sirevaag, A., Kloster, K., Sorteberg, A. and Sandven, S.: Recent wind driven high sea ice area export in the Fram Strait contributes to Arctic sea ice decline, Cryosphere, doi:10.5194/tc-5-821-2011, 2011.

Stephenson, D. B., Pavan, V., Collins, M., Junge, M. M. and Quadrelli, R.: North Atlantic Oscillation response to transient greenhouse gas forcing and the impact on European winter climate: A CMIP2 multi-model assessment, Clim. Dyn., doi:10.1007/s00382-006-0140-x, 2006.

Toudal, L.: Ice extent in the Greenland Sea 1978-1995, Deep. Res. Part II Top. Stud. Oceanogr., doi:10.1016/S0967-0645(99)00021-1, 1999.

Tschudi, M., Meier, W. N., Stewart, J. S., Fowler, C. & Maslanik, J.: Polar Pathfinder Daily 25 km EASE-Grid Sea Ice Motion Vectors, Version 4. Boulder, Colorado USA. NASA National Snow and Ice Data Center Distributed Active Archive Center. Doi: https://doi.org/10.5067/INAWUWO7QH7B. 2019. [Updated 2019]

Tsukernik, M., Deser, C., Alexander, M. and Tomas, R.: Atmospheric forcing of Fram Strait sea ice export: A closer look, Clim. Dyn., 35(7), 1349–1360, doi:10.1007/s00382-009-0647-z, 2010.

Våge, K., Papritz, L., Håvik, L., Spall, M. A. and Moore, G. W. K.: Ocean convection linked to the recent ice edge retreat along east Greenland, Nat. Commun., doi:10.1038/s41467-018-03468-6, 2018.

Vinje, T.: Fram Strait Ice Fluxes and Atmospheric Circulation: 1950-2000, J. Clim., doi:10.1175/1520-0442(2001)014<3508:FSIFAA>2.0.CO;2, 2001.

Visbeck, M., Fischer, J. and Schott, F.: Preconditioning the Greenland Sea for deep convection: ice formation and ice drift, J. Geophys. Res., doi:10.1029/95jc01611, 1995.

Wadhams, P. and Comiso, J. C.: Two modes of appearance of the Odden ice tongue in the Greenland Sea, Geophys. Res. Lett., doi:10.1029/1999GL900502, 1999.

Wadhams, P., Comiso, J. C., Prussen, E., Wells, S., Brandon, M., Aldworth, E., Viehoff, T., Allegrino, R. and Crane, D. R.: The development of the Odden ice tongue in the Greenland Sea during winter 1993 from remote sensing and field observations, J. Geophys. Res. C Ocean., 101(C8), 18213–18235, doi:10.1029/96JC01440, 1996.

Xie, J., Bertino, L., Knut, L. and Sakov, P.: Quality assessment of the TOPAZ4 reanalysis in the Arctic over the period 1991-2013, Ocean Sci., doi:10.5194/os-13-123-2017, 2017.

485 Zamani, B., Krumpen, T., Smedsrud, L. H. and Gerdes, R.: Fram Strait sea ice export affected by thinning: comparing high-
486 resolution simulations and observations, Clim. Dyn., doi:10.1007/s00382-019-04699-z, 2019.

487 Zhang, X., Sorteberg, A., Zhang, J., Gerdes, R. and Comiso, J. C.: Recent radical shifts of atmospheric circulations and rapid
488 changes in Arctic climate system, Geophys. Res. Lett., doi:10.1029/2008GL035607, 2008